

MESOSCALE MODELLING OF REACTION IN HMX-BASED EXPLOSIVES

D.C. Swift and R.N. Mulford
Los Alamos National Laboratory
Los Alamos, New Mexico 87545

R.E. Winter, P. Taylor, D.A. Salisbury and E.J. Harris
AWE Aldermaston
Reading RG7 4PR, U.K.

To give a wide predictive capability, continuum mechanical models of the dynamic loading of explosives should include a representation of the microstructure and chemistry. We have investigated the performance of reactive flow models based on a heterogeneous mixture of components, each of which with its own constitutive model. Time-scales for pressure and temperature equilibration were estimated from the microstructure. Locally, Arrhenius reaction rates were used, with an asymptotic flame front model around grain boundaries. A geometrical model was used to account for the effect of plastic flow around pores. Parameters were deduced for PBX-9501, PBX-9404 and EDC37, all based on HMX, but with different binders and porosities. It was possible to reproduce shock initiation data quite accurately using an Arrhenius barrier close to the value for HMX deduced from calorimetry data, and with a frequency factor close to the frequency for atomic vibrations. Double-shock initiation was also reproduced with reasonable accuracy.

INTRODUCTION

In order to design explosive systems, and to understand the response of explosives to different loading scenarios, reactive flow models must have a wide range of validity. Most experiments to characterize the dynamic response of materials use mechanical diagnostics – pressure gauges, the motion of adjacent materials – so reactive flow models for solid explosives have largely been calibrated against mechanical data and for simplicity have been expressed in terms of mechanical quantities such as pressure and compression. However, at the molecular level it is more natural to express reaction rates in terms of temperature, and mechanically-based reaction rates are unlikely to be able to capture the behavior of an explosive over as wide a range of loading conditions.

Chemical reaction rates vary in a highly non-linear

way with temperature, so the response of a heterogeneous explosive may be dominated not by the average temperature, but by the tail of its spatial variation. A reactive flow model based entirely on the local molecular reaction rate would need to resolve the microstructure of the explosive explicitly. A more efficient approach is to consider asymptotic cases of the correlation between temperature variations and identifiable regions of the microstructure, such as hotspots induced by pore collapse. This model can be regarded as “coarse mesoscale” in the sense that microstructural properties are taken into account in a relatively simple way, and has some features in common with mean-field approaches.

Most solid explosives of technological significance comprise a mixture of different compounds distributed as spatially distinct grains. The dynamical response of an explosive can be correlated with the composition and morphology,

though most reactive flow models are calibrated against each composition and grain size distribution of interest. It is desirable to be able to predict the sensitivity of explosives to variations in composition and morphology over a wide range of loading conditions; this was the objective of the work described here. The approach we took was to cast a continuum-level reactive flow model in terms of the microstructure of the explosive, and including representations of relevant processes which could be justified on physical or chemical grounds. Generally, a different reaction rate was used for each component. Porosity was treated in a straightforward and logical way by including the appropriate proportion of gas in the initial material.

Unfortunately, some of the models needed for a complete description of the behavior do not exist, so we were obliged to compromise between an accurate treatment of processes with missing data, and an approximate treatment of processes with a functional form amenable to sensitivity analysis.

We have previously developed models for nitromethane [1], ammonium nitrate/fuel oil [2], TATB [3,4], and HMX [5], investigating the importance of different physical processes, and making the model gradually more complicated as necessary to explain experimental observations. Here we describe the application of this technique to three HMX-based explosives, spanning significant variations in composition and morphology. This is an extension of our previous work on HMX, with more accurate equations of state and comparing to a wider range of experimental data.

HETEROGENEOUS MIXTURE MODEL

For continuum mechanics simulations, explosive material was represented as a heterogeneous mixture of components. Each component was represented by its volume fraction f_i , a thermodynamically complete equation of state (EOS), and if possible a constitutive model. The continuum mechanics simulation applied a strain field to each element of the problem, which responded with a stress field and changes of its internal state including chemical reactions. The internal response of each element was operator-split from the instantaneous external response: the strain field was applied equally to each component in the mixture, then reactions and the relaxation of imbalances between the pressure and temperature

of each component were calculated for a fixed average strain.

The mixture was allowed to equilibrate in pressure and temperature, with an exponential relaxation rate towards the mean value. Pressure equilibration was assumed to be isentropic.

The time constant τ_p for pressure equilibration was chosen by estimating the characteristic time for sound to pass a few times across a 'typical' grain in the microstructure. For HMX grains a few tens of microns in size, this implies that $\tau_p \sim 0.1 \mu\text{s}$. Estimates of the time constant τ_T for thermal equilibrium from the bulk thermal diffusivity were implausibly large. For practical purposes, they were generally chosen to be an order of magnitude or so larger than τ_p .

The increased plastic flow around internal pores was modeled by simulating the evolution of the state of material adjacent to the pore, as well as its bulk state. The two states were used to characterize the distribution of states in the material. The velocity gradient tensor applied to the pore wall was modeled as

$$\text{grad } \vec{u}_{wall} = \chi(\rho/\rho_0) M \text{grad } \vec{u}_{bulk}$$

where M is a 3×3 strain mapping matrix and $\chi(\rho/\rho_0)$ a compression factor. This model can be used to simulate hotspots originating from shear bands or brittle failure rather than bulk plastic work, by modifying the form of the equation or the values of its parameters. For constant volume compression of a hollow shell,

$$\chi(\rho/\rho_0) = [1 - \rho/\rho_0 (1 - v_0)]^{-1/3}$$

where v_0 is the initial porosity. The strain mapping matrix is set up so that isotropic compression of the bulk material causes a shear component in the compression of the material near the pore, by including non-zero off-diagonal terms. The enhanced plastic strain causes greater heating near the pore than in the bulk material; thermal equilibration is modeled by exponential relaxation to the mean value according to a time constant.

REACTION RATES

Local chemical reaction rates were described by a generalized Arrhenius form:

$$d\lambda/dt = R_0 \exp(-T^*/T) \quad (1)$$

as this form is the most appropriate for chemical processes. Here T^* is the activation energy for reaction, and R_0 is the attempt frequency for effective collisions, which could in principle be used to introduce molecular orientation into the equation. The R_0 and T^* may vary with compression and temperature, but no attempt was made to estimate this variation, and in the present work constants were used. Further investigation of the coefficients in the rate might permit the model to reproduce steric hindrance and other physical phenomena that may limit the activation of a particular chemical reaction [6].

For materials in which a plastic enhancement contribution was included, a weighted average was taken of the Arrhenius reaction rate in the bulk and locally-heated regions.

An additional hotspot term was included, whereby material at the surface of each reactive component i was burnt at the temperature of the adjacent component j . Specifically, the rate used was

$$d\lambda_i/dt = R_0 (\rho_i, T_j) \exp[-T^*(\rho_i, T_j)/T_j] \quad (2)$$

If this ‘‘hotspot rate’’ was high enough to indicate significant reaction over the time interval of integration, the reactive material was consumed in a flame-type process with a flame speed described in principle as a function of density and temperature.

Ideally, the flame speed would be calibrated by microscale simulations of reaction with heat conduction; however, the conduction properties of the explosive components were not known with adequate accuracy. In the present work, we investigated the sensitivity of shock initiation to variations in the flame speed; this was found to be fairly small over plausible values of the speed.

The flame front was applied over the contact area between each appropriate pair of components. The common surface area α_{ij} between each pair of components was estimated from the volume fraction of each using a functional of the volume fractions:

$$\alpha_{ij} \propto f_i^{2/3} f_j^{2/3}. \quad (3)$$

The constant of proportionality was obtained by using the grain size to estimate the number density of grains, and calculating their approximate surface

area between two components for $f_i = f_j = 1/2$. Approximately,

$$\alpha(1/2, 1/2) \propto 4\pi r^2 n$$

where r is the particle diameter in a mixture of two components of equal sizes and n is the number density of particles, estimated from the grain size.

The energy release on reaction was determined from thermodynamic tables of the enthalpy of formation [7,8].

PROPERTIES OF MIXTURE COMPONENTS

The HMX-based explosives considered were PBX-9501, consisting of HMX, estane and BDNPA [9]; PBX-9404, consisting of HMX, nitrocellulose, and CEF [9]; and EDC37, consisting of HMX, K10 (an energetic liquid binder), and nitrocellulose [10].

Little useful data were found on nitrocellulose or the binders, so rough estimates were used. It was found that the heat capacity for large organic molecules could be estimated with reasonable accuracy by assuming that all atoms apart from hydrogens behaved classically; this method was used for nitrocellulose and the binders.

Initial estimates of the Arrhenius parameters were taken from calorimetry data [9], and adjusted to reproduce initiation data. The parameters for HMX were adjusted by considering PBX-9501 data, as this composition does not have a reactive binder. In some simulations, the decomposition of the binder was modelled using a slow Arrhenius process; this made little difference to the initiation behaviour predicted. Initiation was not expected to be sensitive to the flame speed used for hotspot burn. This was verified by sensitivity studies.

Thermodynamically complete EOS for condensed components were estimated from a mechanical EOS (generally obtained from shock wave data) and a constant heat capacity. The isentrope through the STP state was calculated by integrating $p dv$ work using the mechanical EOS. The cold curve was estimated from the isentrope by the procedure used in the Steinberg-Guinan strength model to obtain a melt temperature [11]. An alternative method was to estimate a single point on the cold curve from the thermal expansivity, and use the mechanical EOS to estimate the rest of the

cold curve, again by integrating $p.dv$ work. The approaches gave very similar predictions.

Steinberg's cubic Grüneisen form [12] was used to represent shock data which were non-linear in shock speed – particle speed space. The Grüneisen parameter Γ was estimated from the gradient of the fit in shock speed – particle speed space. For many organic materials, the shock speed often increases rapidly with particle speed at low pressures, implying a large value of Γ . However, this steep gradient has been attributed to a reduction in the free volume between molecules in the liquid [13] and thus may not be represented most accurately by a large Γ . In fact, taking Γ naively from the gradient in this regime often leads to an implausible cold curve. We took a conservative value of Γ in such cases.

HMX

The EOS for HMX was estimated from Hugoniot data [14,15] and thermal properties [9]. An elastic-plastic constitutive model was used, based on observed values of the shear modulus and yield stress [16].

Nitrocellulose

The EOS for nitrocellulose (NC) was estimated by assuming the same Hugoniot data as for cellulose acetate [15] but taking a solid density of 1.65g/cm^3 [17].

Binders

All binders were modeled with the same EOS as polyurethane. The EOS of polyurethane was estimated from Hugoniot data [15] and a “typical” heat capacity for polymers [18].

The constitutive behavior of the binder was treated implicitly by altering the plastic enhancement of deformation in the HMX. The stiffer the binder, the greater the enhancement used.

Reaction products

The products EOS was taken to be that of PBX-9404 in all cases. The initiation properties are unlikely to depend on relatively small differences in the composition and energy of the

products. The Tarver form of the Jones-Wilkins-Lee EOS was used [19]; this form is simple but thermodynamically complete.

Pore gas

Initial porosity was represented by starting with a non-zero volume fraction of the reaction products at the STP state. For CHNO explosives, the mass density and sound speed of the products at STP are close to those of air. Treating the pore gas as products reduces the number of components in the heterogeneous mixture model.

CALIBRATION AND PERFORMANCE FOR HMX-BASED EXPLOSIVES

Previous studies have shown that variations in the reactive behavior of several HMX-based materials arose from differences between binders in the material, indicating that the sensitivity of the explosive was related to the mechanical properties of the constituents. Materials considered here were EDC37, with a soft binder, PBX-9501, with a relatively malleable binder, and PBX-9404, with a stiff binder.

Continuum mechanical calculations were used to simulate shock initiation of the different compositions when subjected to different loading conditions. Simulations were performed by 1D continuum mechanics calculations using a finite difference discretization, Wilkins artificial viscosity to stabilize shock waves, and operator-splitting between continuum mechanics, equilibration and reactions [Mulford99b]. Reaction and equilibration were subcycled, and suppressed when the artificial viscosity was greater than a tenth of the local pressure to prevent unphysical behavior during the passage of the smeared shock. The mesh resolution was 0.5 mm throughout.

PBX-9501

PBX-9501 consists of 95% HMX, 2.5% estane and 2.5% BDNPA by weight, with a porosity of about 1.6% [9]. The binder is fairly soft, so the off-diagonal elements of the mapping matrix were chosen to be $M_{12} = M_{13} = 1$. The equilibration time-scales were chosen from the grain size to be $\tau_p = 0.1 \mu\text{s}$ and $\tau_T = 1 \mu\text{s}$. Reaction of the binder was ignored. The sensitivity of shock initiation to

flame speed was investigated; the result was found to be fairly insensitive for speeds in the range of 0.1 to 1 km/s.

The experimental single-shock run distance to detonation (“Pop plot”) [9] could be reproduced with reasonable accuracy by taking $R_0 = 2 \times 10^7 / \mu\text{s}$ and $T^* = 27000 \text{ K}$ (Fig. 1). This compares quite well with the calorimetry value of 26500 K [9], and R_0 is fairly consistent with frequencies of molecular vibration.

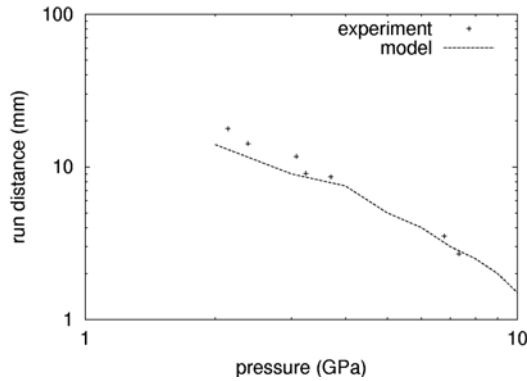


FIGURE 1: POP PLOT FOR PBX-9501.

PBX-9404

PBX-9404 consists of 94% HMX, 3% NC, and 3% CEF by weight, with a porosity of about 1.6% [9]. The binder is relatively stiff, so the off-diagonal elements of the mapping matrix were chosen to be $M_{12} = M_{13} = 2$. The equilibration time-scales were taken to be the same as for PBX-9501. Reaction of the NC and binder were modeled with Arrhenius rates. The NC rate was taken directly from calorimetry, $R_0 = 4.3 \times 10^6 / \mu\text{s}$ and $T^* = 15750 \text{ K}$. The CEF rate was chosen so that decomposition would proceed during a fully-developed detonation, taking $R_0 = 10^8 / \mu\text{s}$ and $T^* = 30000 \text{ K}$.

The predicted Pop plot, which was similar to that for PBX-9501, matched experimental data [9] reasonably well (Fig. 2).

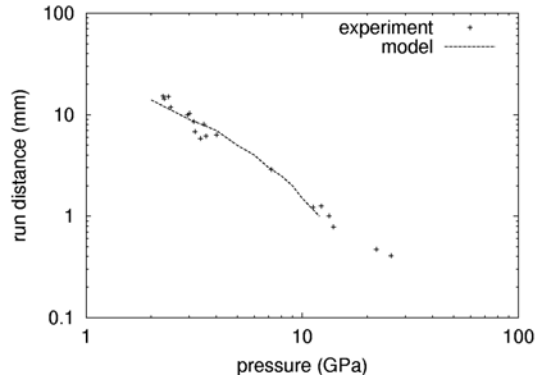


FIGURE 2: POP PLOT FOR PBX-9404.

Pop plots are an integrated measure of the initiation of an explosive, and it is a far more sensitive discriminant to compare the velocity history at different points in the explosive during the build-up to detonation. Experimental measurements have been reported from 1D gun-driven impactor experiments, using electromagnetic gauges to record the particle velocity history at Lagrangian positions in the explosive sample [10].

Simulations were performed of double shock initiation, comparing with experiments in which a gas gun projectile had a low-impedance layer at the front [20]. Comparing with an experiment where the impactor was Vistal with 1.6 mm of PMMA, and was launched at 0.931 km/s, the simulations demonstrated desensitization by the first shock, but the transition to detonation was more abrupt than was observed experimentally (Figs 3 and 4; velocity gauges were at intervals of 1 mm).

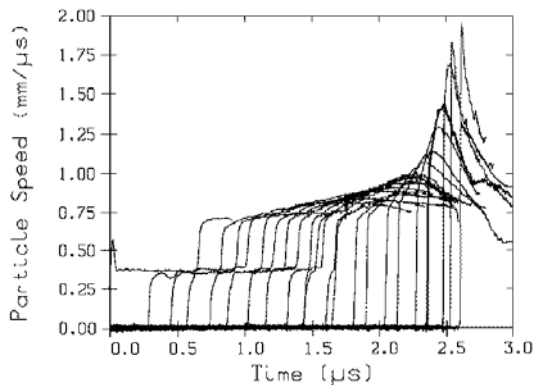


FIGURE 3: VELOCITY GAUGE DATA FOR DOUBLE-SHOCK INITIATION OF PBX-9404.

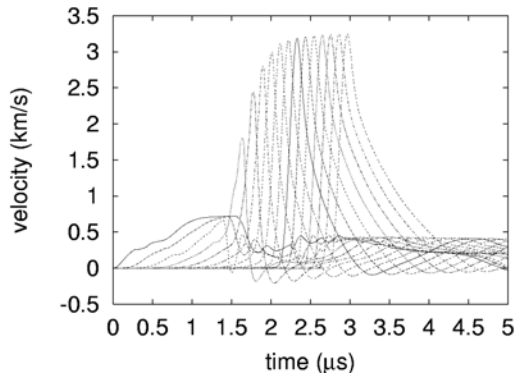


FIGURE 4: PREDICTED VELOCITY GAUGE DATA FOR DOUBLE-SHOCK INITIATION OF PBX-9404.

EDC37

EDC37 consists of 91% HMX, 8% K10, and 1% NC by weight, with a porosity of about 0.18% [10]. The binder is an energetic liquid, so the off-diagonal elements of the mapping matrix were ignored.

With the reaction parameters otherwise unchanged, the predicted Pop plot suggested that EDC37 was more sensitive than is observed experimentally [10]. A reasonable match to the measured Pop plot was obtained by reducing the equilibration time-scales to $\tau_p = 0.01 \mu s$ and $\tau_r = 0.1 \mu s$. This can be justified on the grounds that the pore sizes in EDC37 are much smaller than in the other explosives considered, but it suggests that a better model might be obtained by using the grain sizes directly rather than representing equilibration with a single time-scale. (Fig. 5).

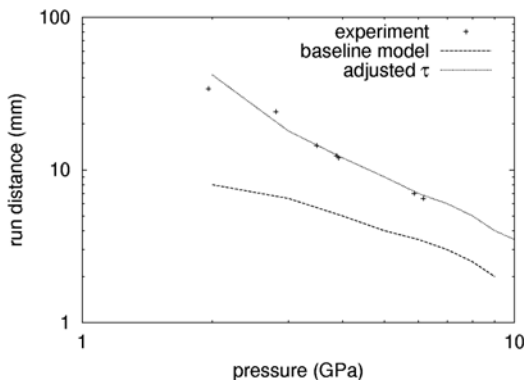


FIGURE 5: POP PLOT FOR EDC37.

Simulations were made of explosively-driven shock initiation experiments, the SI2D design [21]. A cylindrical donor charge, initiated on its axis, was used to drive a shock wave through an attenuating barrier made of steel and then into the sample of EDC37. The EDC37 was confined by a cover plate, allowing a shock to be reflected back into the sample. In shot SI2D/15, where the cover plate was 3 mm of copper, the shock in the EDC37 was not strong enough to cause prompt initiation, and the explosive was desensitized with respect to the reflected shock. It was observed that a significant amount of the chemical energy was imparted as kinetic energy in the cover plate, but that this did not appear to account for the full amount of energy available.

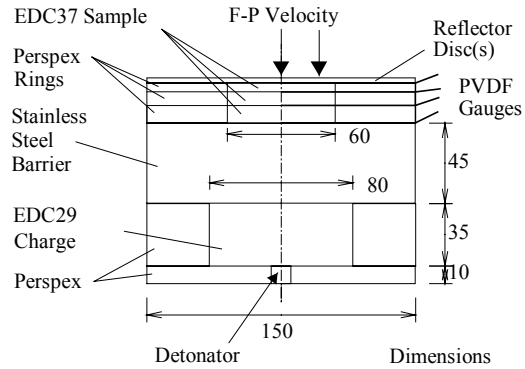


FIGURE 6: SCHEMATIC OF ASSEMBLY FOR SI2D EXPERIMENTS.

The simulations were performed in 1D, approximating the experimental assembly by a spherical geometry centered on the detonator. This representation was found to produce a similar loading history to that measured experimentally using pressure probes near the interface between the barrier and the EDC37 sample. In contrast, the peak pressure induced when the assembly was modeled in 1D plane geometry (i.e. with plane wave initiation rather than a point detonator), the peak pressure at the barrier/sample interface was several times larger. For computational convenience, a simulation was performed of the complete system with the baseline EDC37 model, recording the pressure history at the interface between the donor charge and the barrier. For subsequent calculations, the donor explosive was omitted and the pressure history applied as a boundary condition to the barrier. When comparing experiment and simulation, times in the simulation were offset to bring them into best agreement with the arrival of the shock wave.

With the baseline geometry and the EDC37 reactive flow model deduced from the Pop plot, the peak pressure predicted to occur at the barrier / sample interface was higher than measured experimentally, and the simulations predicted that shock initiation would occur quite promptly in the sample. The behavior of the model was investigated by scaling the applied pressure history. A narrow range of peak drive pressures was found between no significant reaction and prompt initiation. In this region, the predicted pressure history applied to the sample was closer to the experimental data, and the velocity history of the free surface of the cover plate was similar to the measured velocity history. The terminal velocity was slightly too high, suggesting that reactions were quenched slightly too quickly compared with the experiment, though it should be noted that as discussed above the EOS used for the reaction products was not necessarily the most appropriate for this formulation. The agreement obtained was however somewhat better than had been achieved with a Lee-Tarver reaction rate in which the parameters had been adjusted [21]. (Fig. 7.)

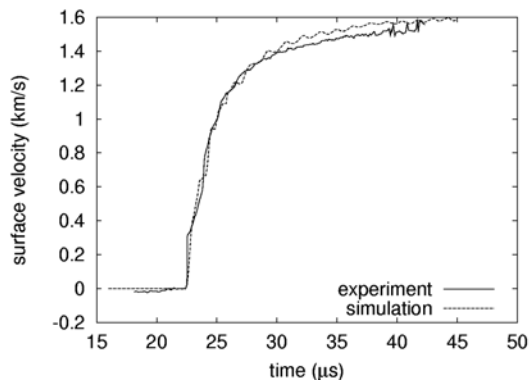


FIGURE 7: MEASURED AND CALCULATED FREE SURFACE VELOCITY FOR SHOT SI2D/15.

DISCUSSION

The reactive flow model performed reasonably well in predicting shock initiation properties over a range of compositions and morphologies for HMX-based explosives. It did not capture some of the detailed initiation behavior, and in particular the simulations predicted too rapid a transition from shock to detonation though it occurred after the correct run distance, for a single or a double shock. This inaccuracy was found to lead to a small but significant discrepancy in metal-driving

performance for reaction following a reflected shock, presumably because the pressure – distance window for slow reactions to occur was too narrow.

There are several possible reasons why a model might behave in this way. It is possible that a single Arrhenius rate is too simplistic, and that for instance the frequency factor or energy barrier change significantly with compression or heating, or that additional reaction steps should be considered – such as a bond-breaking step followed by bond-formation – which might dominate at different stages of the reaction process. Some aspects of this conjecture were investigated by performing simulations in which the Arrhenius rate was artificially limited to different values; this did not appear to widen the window of slow reactions significantly. Another possibility is that the dissipation is greater than estimated for the model, whether in equilibration rates or in the speed of the flame front. Sensitivity studies were also performed for some of the relevant parameters, without finding a better set of values; however, this is a multi-dimensional optimization problem and it is quite possible to miss the best solution. One area which was not studied was the constitutive model of HMX. This was treated as elastic-perfectly plastic, whereas a more accurate model would include strain-rate dependence, thermal softening, and viscosity. In comparison, the elastic-plastic model is likely to over-predict the magnitude of heating from plastic work during pore collapse, which would act to make the model too sensitive.

Although there is scope for performing further sensitivity studies and optimizations, it seems that the model described should be flexible enough to capture many interesting initiation phenomena such as desensitization, as well as offering a predictive capability across compositions and morphologies. The next logical development may be to calibrate the model more carefully against explicit simulations of “representative microstructures” and of course to use better models for the “pure” components where possible. There seems to be no pressing need to adopt more sophisticated distribution functions for material states: to do this consistently with as coherent a representation of a heterogeneous explosive would require not only the distributions but also the correlations between many of the distributions, which is a difficult but necessary component.

CONCLUSIONS

A reactive flow model for heterogeneous explosives was constructed using the properties of the “pure” constituents in an equilibrating mixture. The model included hotspots from pore collapse and the localization of plastic work, and was based on Arrhenius reaction rates, i.e. using temperature as a key parameter. It was possible to reproduce shock initiation data for HMX-based explosives reasonably well with essentially a single set of material parameters, or variations which could be attributed to systematic variations in the microstructure that were over-simplified in the model.

The parameters in the Arrhenius reaction rates were plausible on physical grounds, in that the frequency factor was consistent with atomic vibrations, and the energy barrier agreed fairly well with values obtained from calorimetry experiments. There was a lower degree of consistency when simpler models of the microstructure were used.

ACKNOWLEDGEMENTS

We would like to thank Ron Rabie (Los Alamos National Laboratory) for the benefit of his suggestions on the modeling of nitrocellulose.

REFERENCES

1. R.N. Mulford and D.C. Swift, *Reactive Flow Models for Nitromethane*, in Proc. International Workshop on New Models and Hydrocodes for Shock Wave Processes in Condensed Matter, Edinburgh, Scotland, 19-24 May, 2002 (to appear).
2. R.N. Mulford and D.C. Swift, *Temperature-based reactive flow models for ANFO*, Proc. International Workshop on Non-Ideal Explosives, Socorro, NM, USA, May 2001, EMRTC (2001); see also paper by the Mulford, Braithwaite and Swift at this conference.
3. R.N. Mulford and D.C. Swift, *Reactive flow models for the desensitisation of high explosives*, Proc. International Workshop on Non-Ideal Explosives, held Socorro, New Mexico, USA, Mar 1999, EMRTC (2000).
4. R.N. Mulford and D.C. Swift, *Reactive flow models for the desensitisation of high explosives*, Proc APS Topical Conference on Shock Compression of Condensed Matter, Snowbird, Utah, USA, Jun 1999, AIP (2000).
5. R.N. Mulford and D.C. Swift, Proc APS Topical Conference on Shock Compression of Condensed Matter, Atlanta, GA, USA, 25 to 29 Jun 2001 (to appear).
6. M. Chaudhri and J.E. Field, Proc Roy Soc A340, 113 (1974).
7. Lange's Handbook of Chemistry, 44th Edition
8. K.S. Holian, *T-4 Handbook of Material Properties Data Bases, Vol. 1 c: Equations of State*, Los Alamos National Laboratory report LA-10160-MS (1984).
9. T.R. Gibbs and A. Popolato, “LASL Explosive Property Data”, University of California Press, Berkeley (1980).
10. R.L. Gustavsen, S.A. Sheffield, R.R. Alcon, L.G. Hill, R.E. Winter, D.A. Salisbury and P. Taylor, *Initiation of EDC37 measured with embedded electromagnetic particle velocity gauges*, Proc. APS SCCM 1999, AIP (1999).
11. D.J. Steinberg, *Equation of State and Strength Properties of Selected Materials*, Lawrence Livermore National Laboratory report UCRL-MA-106439 change 1 (1996).
12. D.C. Swift, *Steinberg-Style Grüneisen Equations of State for Cerium, Lanthanum and Scandium*, Los Alamos National Laboratory report LA-UR-01-3005 (2001).
13. J.N. Fritz (Los Alamos National Laboratory), private communication (2001).
14. M. van Thiel, *Compendium of Shock Wave Data*, Lawrence Radiation Laboratory report UCRL-50108 (1966).
15. S.P. Marsh (Ed), “LASL Shock Hugoniot Data”, University of California (1980).
16. J.J. Dick, A.R. Martinez and R.S. Hixson, *Plane impact response of PBX-9501 below 2 GPa*, Proc. 11th International Detonation Symposium, ONR~33300-5 (2000).
17. R. Rabie (Los Alamos National Laboratory), private communication (2001).
18. J.A. Dean, “Lange's Handbook of Chemistry” (13th ed.), McGraw-Hill (1972).
19. P.C. Souers and L.C. Haselman Jr, *Detonation equation of state at LLNL*, Lawrence Livermore National Laboratory report UCRL-ID-116113 (1994).
20. R.N. Mulford (Los Alamos National Laboratory), unpublished gas gun data.
21. P. Taylor, D.A. Salisbury, L.S. Markland, R.E. Winter and M.I. Andrew, *Reaction of shocked but undetonated HMX-based explosive*, Proc APS Topical Conference on Shock Compression of Condensed Matter, Atlanta, GA, USA, 25 to 29 Jun 2001 (to appear).

